Experimental investigation of creep behavior of clastic rock in Xiangjiaba Hydropower Project

Yu Zhang [a,b,*], Wei-ya Xu [b], Jian-fu Shao [b], Hai-bin Zhao [c], Wei Wang [b]

[a] *College of Pipeline and Civil Engineering, China University of Petroleum, Qingdao 266555, PR China*
[b] *Geotechnical Research Institute, Hohai University, Nanjing 210098, PR China*
[c] *Hunan Provincial Key Laboratory of Key Technology on Hydropower Development, Changsha 410014, PR China*

Abstract

There are many fracture zones crossing the dam foundation of the Xiangjiaba Hydropower Project in southwestern China. Clastic rock is the main media of the fracture zone and has poor physical and mechanical properties. In order to investigate the creep behavior of clastic rock, triaxial creep tests were conducted using a rock servo-controlling rheological testing machine. The results show that the creep behavior of clastic rock is significant at a high level of deviatoric stress, and less time-dependent deformation occurs at high confining pressure. Based on the creep test results, the relationship between axial strain and time under different confining pressures was investigated, and the relationship between axial strain rate and deviatoric stress was also discussed. The strain rate increases rapidly, and the rock sample fails eventually under high deviatoric stress. Moreover, the creep failure mechanism under different confining pressures was analyzed. The main failure mechanism of clastic rock is plastic shear, accompanied by a significant compression and ductile dilatancy. On the other hand, with the determined parameters, the Burgers creep model was used to fit the creep curves. The results indicate that the Burgers model can exactly describe the creep behavior of clastic rock in the Xiangjiaba Hydropower Project.

1. Introduction

The time-dependent (creep) behavior of rock refers to the continued deformation under the effects of constant stress, including deformations, slips, and failures (Sun, 2007; Ma, 2004; Brantut et al., 2013). It is one of the most important mechanical properties of rock material, and can be considered an important basis for explaining and analyzing the phenomena of geological tectonic movement, as well as predicting long-term stability for rock engineering (Tsai et al., 2008; Yang and Jiang, 2010; Zhang et al., 2013). Therefore, the time effect of geotechnical engineering stability is increasingly considered. Taking into account delayed deformations, it is considered that failure can take place over a large span of time in many geotechnical projects (Bayraktar et al., 2009; Yin et al., 2013; Yang et al., 2014). A lot of deformation failures and losses of stability in geotechnical projects are not instances of transient destruction, but develop over time (Dusseault and Fordham, 1993; Boukharov et al., 1995; Damjanac and Fairhurst, 2010). Deformation of the dam foundations and abutments can last for several decades, and creep failure of rock tunnels can occur after construction for several decades (Fan, 1993; Gudmundsson et al., 2010; Zhang et al., 2012, 2014b). Therefore, it is essential to study the creep properties of rocks.

Laboratory testing is the most important method of studying rock mechanical properties (Maranini and Brignoli, 1999;

* Corresponding author.
E-mail address: zhangyuhohai@gmail.com (Yu Zhang).
Peer review under responsibility of Hohai University.

Li and Xia, 2000). It is also used to analyze rock creep constitutive relations and parameters meant to evaluate the long-term stability of rock engineering (Dahou et al., 1995; Pietruszczak et al., 2002; Barla et al., 2012). Many achievements in the experimental study of creep behavior of different types of rocks have been made in China and other countries. Based on a number of uniaxial and triaxial creep test results, the effects of confining pressure and axial pressure on the creep stress-strain behavior of salt rock were analyzed by Yang et al. (1999), and an exponential function was suggested to model the creep strain from transient to steady states. Carter et al. (1993) investigated the influence of temperature on creep behavior and found that the time-dependent properties of salt rock were strongly dependent on temperature. Chan et al. (1997) reported a large number of uniaxial and triaxial test results and analyzed the confining pressure effects on the creep strain. Li et al. (2008) studied the relation of complete creep processes and triaxial stress-strain curves of rocks. Fabre and Pellet (2006) demonstrated the creep behavior of three kinds of rocks characterized by a high proportion of clay particles, and the viscosity of these sedimentary rocks was studied under different loading conditions. However, concerning the study of creep mechanical properties of rocks in some specific projects such as hydropower projects, little experimental data have been reported.

There are many existing large-scale hydropower projects in southwestern China, which create severe challenges for experiments and the theoretical and numerical research on the creep behavior of rocks and long-term stability of rock engineering. This study focused on the creep behavior of the clastic rock core from the Limeiwan fracture zone in the dam foundation of the Xiangjiaba Hydropower Project, which is located on the lower pool of the Jinsha River, at the border of Sichuan and Yunnan provinces. The dam is a concrete gravity dam with a maximum height of 161 m and a length of 909 m. The fracture zone crosses the dam foundation, and the area and thickness of the fracture zone are relatively large (Fig. 1). Clastic rock is the main media of the fracture zone and it has poor physical and mechanical properties. The creep mechanical behavior of such rock has an important impact on the long-term stability of engineering structures and should be investigated carefully. This paper presents the results of triaxial creep tests on this clastic rock. Based on creep experiments under different confining pressures, the creep constitutive relation and parameters have been determined.

2. Lithologic characteristics and experimental program

2.1. Lithologic characteristics of rock samples

The clastic rock materials were obtained from the T^3_{2-6} sub-petrofabric in the fracture zone in cataclastic and clastic shapes (Fig. 2). They were soft rocks with poor integrity, which were highly weathered and had the characteristics of low specific gravity, medium porosity, loose organizational structure, and high moisture content. The results of basic physical property tests showed that the averages of natural
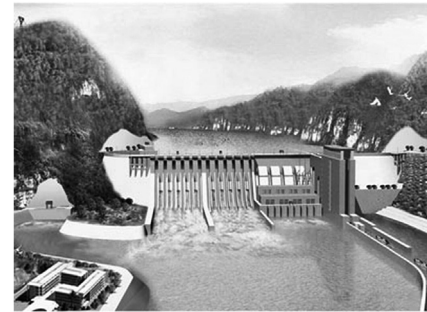
(a) Sketch of Xiangjiaba Dam
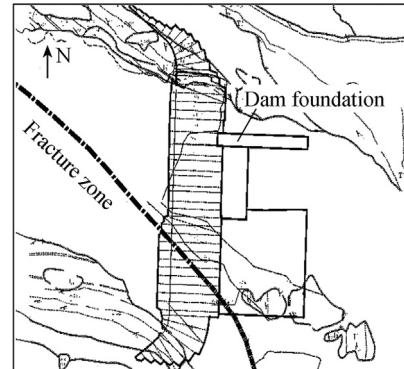
(b) Geological distribution of fracture zone

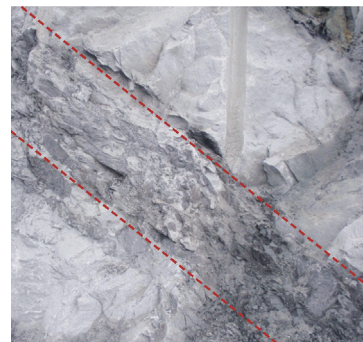Fig. 1. Xiangjiaba Hydropower Project and fracture zone in dam foundation.

Fig. 2. Geological distribution of clastic rock in Xiangjiaba Hydropower Project.

density and dry density were 2.375 g/cm^3 and 2.225 g/cm^3, respectively. The averages of moisture content and porosity were 6.59% and 18.23%, respectively. Furthermore, the flow behavior showed that the permeability coefficient varied from 0.14×10^{-5} to 16.3×10^{-5} cm/s in the natural state, and its values were almost the same in the directions parallel and perpendicular to the bedding plane. In view of this, it can be concluded that at the sample scale, the rock was mid-permeable with isotropic permeability (Zhang et al., 2014a).

Optical microscopic tests were performed to analyze the microstructure and mineral composition of the clastic rock (Fig. 3). The results indicated that the clastic rock retained fine-grained texture with an extremely complex microstructure. Also, the main mineral composition consisted of quartz, chalcedony, feldspar (K-feldspar and plagioclase), sericite, chlorite, a small amount of iron compounds, and trace
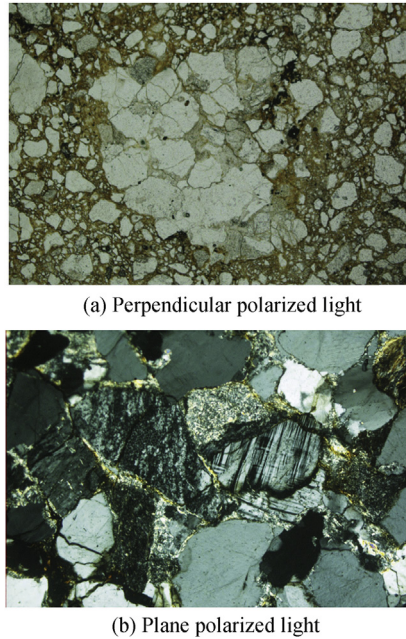
(a) Perpendicular polarized light

(b) Plane polarized light

Fig. 3. Optical microscopic test results of clastic rock sample.

Fig. 4. Typical compression stress-strain curves under different confining pressures.

minerals. The trace minerals mainly included tourmaline, zircon, phosphorites, zoisite, and glauconite. The main chemical constituent was SiO_2 (accounting for 80.75%−83.52%), followed by Al_2O_3, and a small amount of mixture of Fe_2O_3, CaO, and MgO.

2.2. Test equipment and procedure

The experiments were performed with the rock servo-controlling rheological testing machine (Zhang et al., 2014b). This equipment can be used to carry out conventional compression tests and rheological tests such as uniaxial creep tests and triaxial creep tests. The confining pressure ranged from 0 to 60 MPa, and the maximum deviatoric stress could reach 500 MPa. The multi-step loading method was adopted in axial loading, with steps ranged from 4 to 6. The temperature and humidity were kept constant during all tests. The samples were standard cylindrical, 50 mm in diameter and 100 mm in height. Due to the poor quality of some rock samples, extreme care was necessary in handling of the samples, and some special preparations were required. For instance, the samples were stored with a sealing technique. The same test procedures were described in Zhang et al. (2013).

3. Behavior of conventional triaxial compression tests

In order to confirm multi-step stress levels of triaxial creep tests, conventional triaxial compression tests on clastic rock samples under the confining pressures of 1.0 MPa, 1.5 MPa, and 2.0 MPa were carried out first. Typical conventional compression stress-strain curves of the clastic rock are shown in Fig. 4, where σ and ε are the deviatoric stress and strain of rock, respectively, and mechanical parameters are listed in Table 1. The stress-strain curves show approximate plastic platforms when the strain exceeds a limit value. It is also
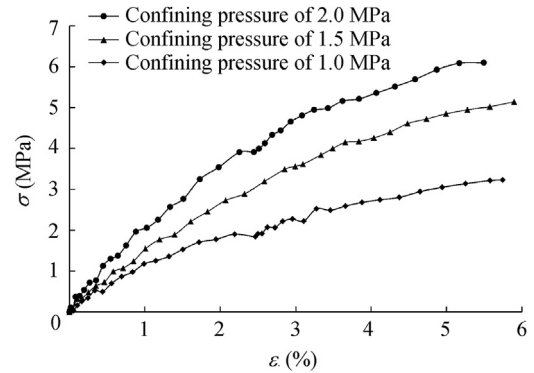
worthwhile to point out that the sample fails when the axial strain exceeds 5.0%, which is much larger than that for hard rock. We can conclude that the peak strength increases gradually with the confining pressure. It can be seen that the sample is not at an obvious stage of crack closure.

In general, the response can be decomposed into four phases for all tests. During the initial loading, a quasi-linear and reversible stress-strain relation is obtained, indicating the elastic compressibility of the rock skeleton, and the elastic modulus can be determined from the slope of the stress-strain curve in this phase. When the stress reaches a certain value, called the yield stress, a nonlinear plastic phase is observed, with significant increase of strain, and the slope of the curve decreases. Under different confining pressures, nonlinear behavior begins at axial strains of about 1.0%. With the incremental stress, a general strain-hardening phase is produced with the increase of the contact surface among grains. Followed by a large axial strain, the phase of plastic failure occurs, in which cracks coalesce. These phases are similar to plastic consolidation in soil mechanics. Due to the hardening behavior of stress-strain curves of the clastic rock, the deformation modulus is slightly lower than the elastic modulus. The deformation modulus of the rock sample has a close relation with the nonlinear deformation under primary loading.

4. Results of triaxial creep tests

4.1. Analysis of creep strain

Triaxial creep tests were performed at ambient temperatures of (20.0 ± 1.5) °C. The confining pressures in the creep tests were the same as those in the conventional triaxial compression tests. Under the confining pressure of 1.0 MPa, the deviatoric stresses of 1.00, 1.50, 2.50, and 3.00 MPa were

Table 1

Conventional mechanical parameters of compression tests of clastic rock (MPa).

Confining pressure	Peak strength	Elastic modulus	Deformation modulus
1.0	3.23	115.4	72.5
1.5	5.12	142.5	118.0
2.0	6.10	212.5	153.8

selected, while under the confining pressures of 1.5 and 2.0 MPa, the deviatoric stress was increased by 0.75 MPa per step from 1.00 to 4.75 MPa until failure of laboratory samples occurred. At each loading step, the deviatoric stress was kept constant for a time interval of more than 48 h with the axial strain continuously recorded.

The axial strain-time curves under different confining pressures are presented in Fig. 5. Creep curves are smooth without fluctuation, indicating that the creep strain has continuity over time. The results show that at a low deviatoric stress level, the axial creep strain is unnoticeable, while the creep phenomenon of the clastic rock becomes significant with the increase of the deviatoric stress. The main feature associated with the failure is the high axial plastic strain as well as the high strain rate due to long-term accumulation of creep effects. Therefore, no brittle damage is observed in the rock samples.

As shown in Fig. 5(a), under the confining pressure of 1.0 MPa, when the deviatoric stress is less than 2.5 MPa, the

creep strain is unnoticeable. When the deviatoric stress increases to 2.5 MPa, the increment of axial creep strain is 0.71%. When the deviatoric stress reaches 3.00 MPa, the creep strain is greater than at previous stress levels. After five hours of constant loading, the creep strain increases by 0.83%, and, eventually, the rock sample fails via the large creep strain.

As shown in Fig. 5(b), under the confining pressure of 2.0 MPa, when the deviatoric stress is less than 3.25 MPa, the creep strain is unnoticeable. When the deviatoric stress reaches 4.75 MPa, the creep strain increases more quickly than before. After three hours of constant loading, the creep strain increases by 0.82%, and the rock sample fails eventually. In general, the confining pressure has a significant influence on the creep strain of rock samples. Under the same condition, the greater the confining pressure is, the lesser the corresponding creep strain will be.

4.2. Analysis of creep strain rate

It can be deduced from Fig. (5) that for a certain value of the deviatoric stress, the strain rate increases first and then gradually decreases to a constant value after a period of time. According to the evolution of the creep strain rate, the creep curve can be divided into transient and steady stages. The creep strain rate tends to be a value close to zero at low deviatoric stress. At high deviatoric stress, the evolution of the creep strain rate is similar to its performance at low deviatoric stress, but the value is greater. Under the confining pressure of 2.00 MPa, the creep strain rate tends to be a constant value of $0.8 \times 10^{-3} h^{-1}$ at a deviatoric stress of 1.0 MPa, and the value increases to $5.53 \times 10^{-3} h^{-1}$ at a deviatoric stress of 4.00 MPa. After the stress of 4.75 MPa is applied at the last loading step, the strain rate significantly increases until the rock sample fails, and the process lasts about three hours. Therefore, the strain rate increases with the deviatoric stress.

4.3. Creep failure mode and mechanism

The creep failure patterns under different confining pressures are shown in Fig. 6. The main failure mechanism of the rock sample is plastic shear accompanied by a significant compression and ductile dilatancy. Sample failure is classically produced by the pore compression and crack coalescence. It can be said that the essential failure is the result of synthetic effects of the material defects, heterogeneity, and long-term accumulation of microcrack damage. Under time and loading effects, micromovement is caused by the crystal displacement and mineral cleavage. Thus, the rock deformation includes the diffusion of lattice dislocations, crack expansion, and compatible deformation among grains. The rock has different scales of initial microdefects, such as fissures, joints, dislocations, etc., which determine the macroscopic behavior of the rock. It is very easy for microdefects to develop and dislocate between grains and cleavages under constant loading. Then, ductile deformation accompanied by moderate dilation or even compaction results in a number of small macrocracks on the sample surface.
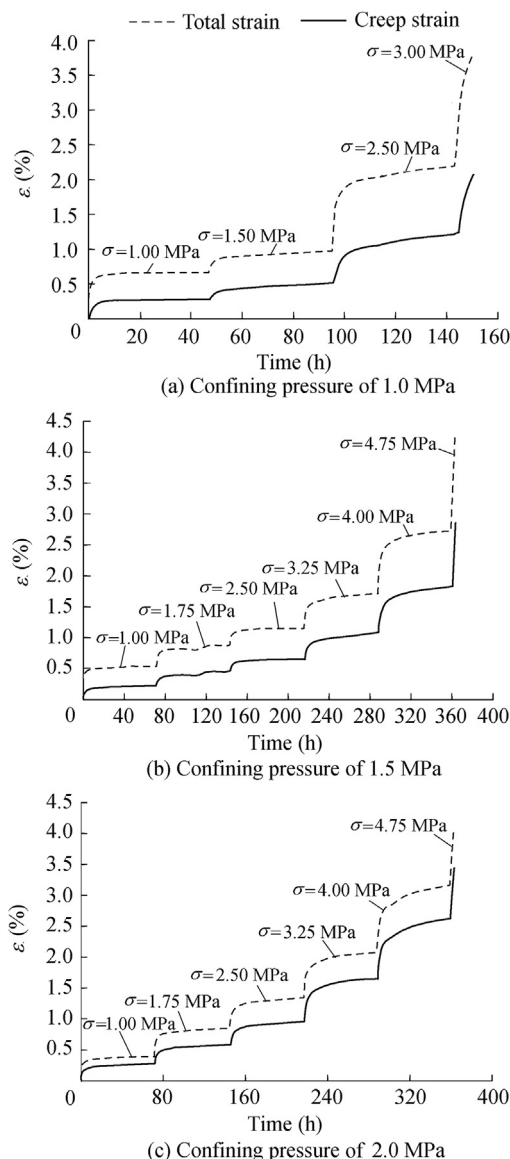

Fig. 5. Relation between creep strain and time under different confining pressures.

(a) Confining pressure of 1.0 MPa
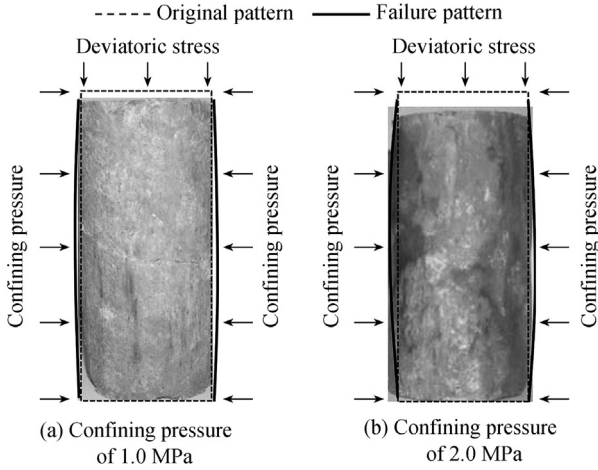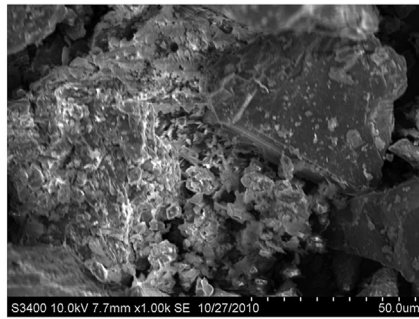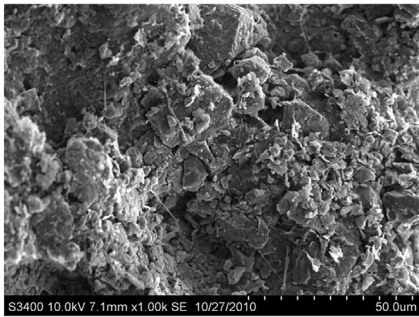
(b) Confining pressure of 2.0 MPa

Fig. 6. Typical creep failure patterns of clastic rock.

Based on the microscale and mesoscale analyses, this section discusses the shapes of internal microdefects after creep failure. The samples were selected along the surface of the fracture zone in this study. From the scanning electron microscope (SEM) observations (Fig. 7), it can be seen that the microscopic failure patterns are slightly different under various confining pressures. There are more growing cracks, and the fracture surface is coarse with less micro grains under low confining pressures. With the increase of the confining pressure, the porosity decreases with more micro grains on the fracture surface. During the testing process, microfissure damage inside the rock sample continuously accumulates, and then, the cracks, originating from the defects of initial internal

(a) Confining pressure of 1.0 MPa

(b) Confining pressure of 2.0 MPa

Fig. 7. SEM observations of rock samples after creep failure at magnification of 1 000.

voids, extend and interpenetrate, and eventually lead to the failure.

5. Creep model and parameter identification

The creep curves in Fig. 5 show that the clastic rock sample experiences a transient creep stage and a steady creep stage under each step of loading, and the creep strain rate first increases and then decreases toward a constant value. According to the creep behavior shown by these curves, the Burgers creep model, which can be regarded as the combination of the Maxwell model and Kelvin model, was chosen to describe those results (Fig. 8).
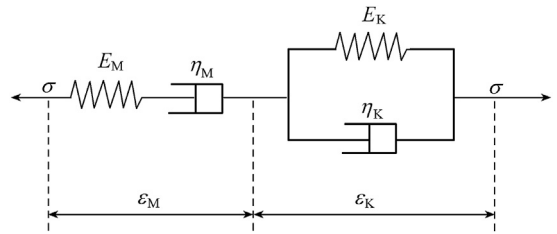

Fig. 8. Illustration of Burgers creep model.

The constitutive equation of the Burgers creep model is as follows:

$$\begin{cases} \sigma_M = E_M \varepsilon_M = \eta_M \dot{\varepsilon}_M \\ \sigma_K = E_K \varepsilon_K + \eta_K \dot{\varepsilon}_K \\ \sigma = \sigma_M = \sigma_K \\ \varepsilon = \varepsilon_M + \varepsilon_K \end{cases} \quad (1)$$

where σ_M, ε_M, and $\dot{\varepsilon}_M$ are the deviatoric stress, strain, and strain rate of the Maxwell body, respectively; σ_K, ε_K, and $\dot{\varepsilon}_K$ are the deviatoric stress, strain, and strain rate of the Kelvin body, respectively; E_M and η_M are the elastic modulus and viscosity coefficient of the Maxwell body; and E_K and η_K are the elastic modulus and viscosity coefficient of the Kelvin body.

Using the Laplace transform to solve Eq. (1), the corresponding creep constitutive equation can be expressed:

$$\varepsilon = \frac{\sigma}{E_M} + \left(\frac{\sigma}{\eta_M}\right)t + \frac{\sigma}{E_K}\left(1 - e^{-\frac{E_K}{\eta_K}t}\right) \quad (2)$$

The data measured under multi-step loading in the test were processed using Boltzmann superposition (Zhang, 2012). In order to determine creep mechanical parameters at different deviatoric stresses, an iteration procedure was used based on the Quasi-Newton search method. The relevant parameters of the Burgers creep model were identified from data processing, as shown in Table 2, and the fitted curves could be obtained with the required precision. Through analysis of the obtained creep mechanical parameters (Table 2), it can be determined that the Burgers model parameters vary with the deviatoric stress and the time-dependent deformation of the clastic rock increases with the long-term constant deviatoric stress.

Table 2
Creep parameters of clastic rock under different confining pressures.

| Confining pressure (MPa)	Deviatoric stress (MPa)	Burgers model parameter			
		E_M (GPa)	E_K (GPa)	η_M (GPa·h)	η_K (GPa·h)
1.00	1.00	0.20	67.05	0.25	0.81
	1.50	0.22	62.95	0.62	0.93
	2.50	0.24	36.30	0.30	0.32
	3.00	0.14	47.33	0.38	0.47
1.50	1.00	1.25	98.24	0.61	0.58
	1.75	0.32	112.08	0.78	0.66
	2.50	0.28	172.06	1.01	1.02
	3.25	0.28	140.96	0.83	0.97
	4.00	0.23	108.47	0.84	0.79
	4.75	0.17	100.48	0.92	0.69
2.00	1.00	1.60	72.65	0.33	0.23
	1.75	0.48	136.71	0.59	0.44
	2.50	0.29	124.41	0.73	0.63
	3.25	0.25	104.48	0.72	1.11
	4.00	0.19	72.72	0.70	1.55
	4.75	0.16	30.09	1.39	1.10

As shown in Table 2, under the confining pressures of 1.5 MPa and 2.0 MPa, the elastic modulus E_M is high at the first deviatoric stress. Then, E_M gradually decreases with the increase of the deviatoric stress. The rock is linear elastic in this stage. When the deviatoric stress increases to a certain value, the rock sample enters the plastic phase and, at this stage, eventually fails. During this stage, E_M shows a further decrease. Therefore, by analyzing the evolutions of E_M, we observe that the degradation of the elastic modulus is decelerated with the increase of the deviatoric stress, and the value of E_M varies by a power function with the deviatoric stress during creep tests (Fig. 9(a)). Because of the high heterogeneity of the rock sample, the evolution of the elastic modulus is insignificant under the confining pressure of 1.0 MPa.

The viscosity coefficient η_M can reflect the variation of the strain rate of steady creep. Generally, the strain rate of this stage is quasi-independent of the loading history and depends only on the current stress state (Yang et al., 1999). As shown in Table 2, η_M demonstrates an overall increasing trend with the deviatoric stress, indicating that the strain rate of steady creep continues to increase until the deviatoric stress reaches its maximum. The relationships between η_M and deviatoric stress can also be expressed by a power function (Fig. 9(b)). E_K/η_K reflects the duration from the transient creep to steady creep. It takes the rock more time to reach a steady state when E_K/η_K is lower. Results show that relationship between E_K/η_K and deviatoric stress can be expressed by an exponential function (Fig. 9(c)).

The comparison between the Burgers model's predictions of creep curves and tested creep results under different confining pressures is shown in Fig. 10. The Burgers model can describe well the time-dependent behavior of the clastic rock as well as transient and steady creeps.
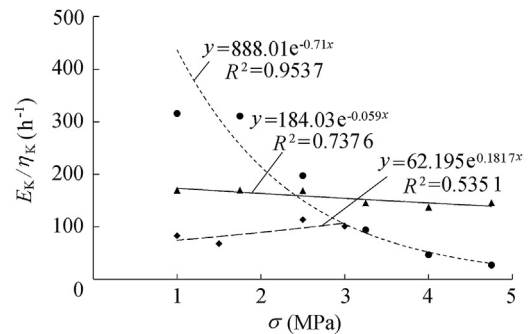
6. Conclusions

(1) The creep behavior of clastic rock is not significant at low deviatoric stress. However, at high deviatoric stress, the creep behavior is very significant, and the time-dependent
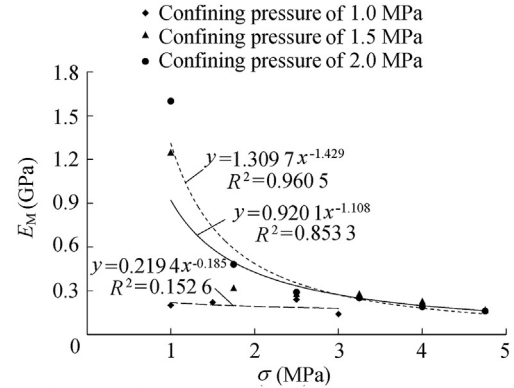
(a) Relationship between parameter E_M and deviatoric stress σ
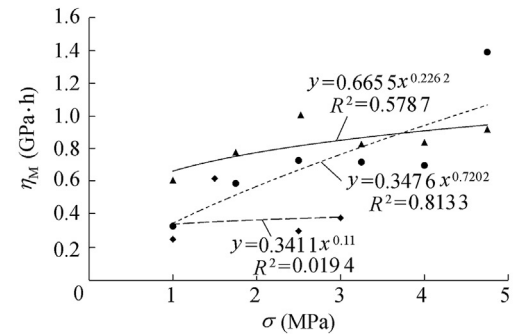
(b) Relationship between parameter η_M and deviatoric stress σ

(c) Relationship between E_K/η_K ratio and deviatoric stress σ

Fig. 9. Relations between Burgers model parameters and deviatoric stress.

deformation is large. Two creep phases, the transient and steady stages, appear to a significant degree when the deviatoric stress is high. The time-dependent deformation decreases with the increase of the confining pressure, indicating that less creep of the rock sample may occur at high confining pressure.

(2) The creep strain rate of the rock sample varies with the deviatoric stress. The strain rate tends to be a value close to zero over time at low deviatoric stress. However, the strain rate increases with the deviatoric stress. When the deviatoric stress is increased to a certain value, the strain rate increases rapidly, and the rock sample fails eventually.

(3) The main failure mechanism of clastic rock is plastic shear, accompanied by a significant compression and ductile dilatancy. The failure may be due to the occurrence, development, and coalescence of microcracks under long-term constant stresses. As shown by SEM experiments, creep
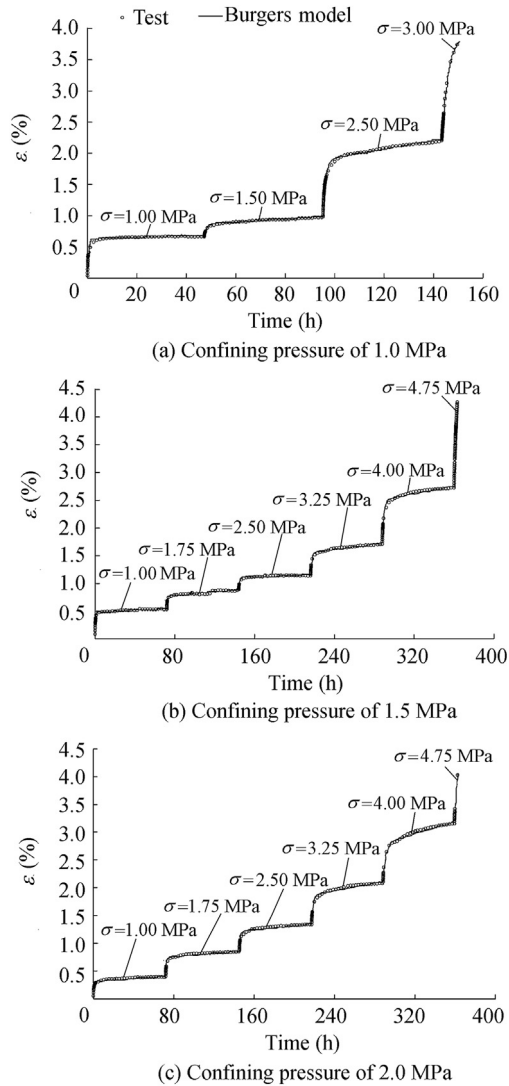
Fig. 10. Comparison between Burgers model's prediction of creep curves and tested results.

strains and microscopic failure patterns are different under different confining pressures. The reason is that the micro-fissure damages inside the rock sample continuously accumulate in the process of creep testing.

(4) Based on the tested results, the creep parameters of the Burgers creep model are determined through curve fitting of measured data. The results demonstrate a high precision of the Burgers creep model in prediction of the creep curve as compared with the measured curve. Thus, the model can describe the overall time-dependent behavior of clastic rock. It can provide a basis for creep numerical simulation, which is vital for predicting the long-term stability of the Xiangjiaba Hydropower Project.

References

Barla, G., Debernardi, D., Sterpi, D., 2012. Time-dependent modeling of tunnels in squeezing conditions. Int. J. Geomech. 12 (6), 697−710. http://dx.doi.org/10.1061/(ASCE)GM.1943-5622.0000163.

Bayraktar, A., Kartal, M.E., Basaga, H.B., 2009. Reservoir water effects on earthquake performance evaluation of Torul Concrete-faced Rockfill Dam. Water Sci. Eng. 2 (1), 43−57. http://dx.doi.org/10.3882/j.issn.1674-2370.2009.01.005.

Boukharov, G.N., Chanda, M.W., Boukharov, N.G., 1995. The three processes of brittle crystalline rock creep. Int. J. Rock Mech. Min. Sci. 32 (4), 325−335. http://dx.doi.org/10.1016/0148-9062(94)00048-8.

Brantut, N., Heap, M.J., Meredith, P.G., Baud, P., 2013. Time-dependent cracking and brittle creep in crustal rocks: a review. J. Struct. Geol. 52, 17−43. http://dx.doi.org/10.1016/j.jsg.2013.03.007.

Carter, N.L., Horseman, S.T., Russell, J.E., Handin, J., 1993. Rheology of rocksalt. J. Struct. Geol. 15 (9−10), 1257−1271. http://dx.doi.org/10.1016/0191-8141(93)90168-A.

Chan, K.S., Bodner, S.R., Fossum, A.F., Munson, D.E., 1997. A damage mechanics treatment of creep failure in rock salt. Int. J. Damage Mech. 6 (2), 122−152. http://dx.doi.org/10.1177/105678959700600201.

Dahou, A., Shao, J.F., Bederiat, M., 1995. Experimental and numerical investigations on transient creep of porous chalk. Mech. Mater. 21 (1), 147−158. http://dx.doi.org/10.1016/0167-6636(95)00004-6.

Damjanac, B., Fairhurst, C., 2010. Evidence for a long-term strength threshold in crystalline rock. Rock Mech. Rock Eng. 43 (5), 513−531. http://dx.doi.org/10.1007/s00603-010-0090-9.

Dusseault, M.B., Fordham, C.J., 1993. Time dependent behaviour of rocks. In: Comprehensive Rock Engineering: Principles, Practice and Projects. Pergamon Press, Oxford, pp. 119−149.

Fabre, G., Pellet, F., 2006. Creep and time-dependent damage in argillaceous rocks. Int. J. Rock Mech. Min. Sci. 43 (6), 950−960. http://dx.doi.org/10.1016/j.ijrmms.2006.02.004.

Fan, G.Q., 1993. Rheological Mechanics of Geotechnical Engineering. China Coal Industry Publishing House, Beijing (in Chinese).

Gudmundsson, A., Simmenes, T.H., Belinda, L., Sonja, L.P., 2010. Effects of internal structure and local stresses on fracture propagation, deflection, and arrest in fault zones. J. Struct. Geol. 32 (11), 1643−1655. http://dx.doi.org/10.1016/j.jsg.2009.08.013.

Li, Y.P., Wang, Z.Y., Tang, M.M., Wang, Y., 2008. Relations of complete creep processes and triaxial stress-strain curves of rock. J. Cent. South Univ. Technol. 15 (1), 311−315. http://dx.doi.org/10.1007/s11771-008-0370-7.

Li, Y.S., Xia, C.C., 2000. Time-dependent tests on intact rocks in uniaxial compression. Int. J. Rock Mech. Min. Sci. 37 (3), 467−475. http://dx.doi.org/10.1016/S1365-1609(99)00073-8.

Ma, L., 2004. Experimental Investigation of Time Dependent Behavior of Welded Topopah Spring Tuff. Ph. D. dissertation. University of Nevada, Reno.

Maranini, E., Brignoli, M., 1999. Creep behaviour of a weak rock: experimental characterization. Int. J. Rock Mech. Min. Sci. 36 (1), 127−138. http://dx.doi.org/10.1016/S0148-9062(98)00171-5.

Pietruszczak, S., Lydzba, D., Shao, J.F., 2002. Modelling of inherent anisotropy in sedimentary rocks. Int. J. Solids Struct. 39 (3), 637−648. http://dx.doi.org/10.1016/S0020-7683(01)00110-X.

Sun, J., 2007. Rock rheological mechanics and its advance in engineering applications. Chin. J. Rock Mech. Eng. 26 (6), 1081−1106 (in Chinese).

Tsai, L.S., Hsieh, Y.M., Weng, M.C., Huang, T.H., Jeng, F.S., 2008. Time-dependent deformation behaviors of weak sandstones. Int. J. Rock Mech. Min. Sci. 45 (2), 144−154. http://dx.doi.org/10.1016/j.ijrmms.2007.04.008.

Yang, C.H., Daemen, J.J.K., Yin, J.H., 1999. Experimental investigation of creep behavior of salt rock. Int. J. Rock Mech. Min. Sci. 36 (2), 233−242. http://dx.doi.org/10.1016/S0148-9062(98)00187-9.

Yang, S.Q., Jiang, Y.Z., 2010. Triaxial mechanical creep behavior of sandstone. Min. Sci. Technol. 20 (3), 339−349. http://dx.doi.org/10.1016/S1674-5264(09)60206-4.

Yang, W.D., Zhang, Q.Y., Li, S.C., Wang, S.G., 2014. Time-dependent behavior of diabase and a nonlinear creep model. Rock Mech. Rock Eng. 47, 1211−1224. http://dx.doi.org/10.1007/s00603-013-0478-4.

Yin, D.S., Li, Y.Q., Wu, H., Duan, X.M., 2013. Fractional description of mechanical property evolution of soft soils during creep. Water Sci. Eng. 6 (4), 446−455. http://dx.doi.org/10.3882/j.issn.1674-2370.2013.04.008.

Zhang, Y., 2012. Experimental Investigation on Rheological Mechanics of Dam Foundation Deflection Zone Cataclastic Rock and its Study of Constitutive Model. Ph. D. dissertation. Hohai University, Nanjing (in Chinese).

Zhang, Y., Xu, W.Y., Gu, J.J., Wang, W., 2013. Triaxial creep tests of weak sandstone from the deflection zone of high dam foundation. J. Cent. South Univ. Technol. 20 (9), 2528−2536. http://dx.doi.org/10.1007/s11771-013-1765-7.

Zhang, Y., Shao, J.F., Xu, W.Y., Zhao, H.B., Wang, W., 2014a. Experimental and numerical investigations on strength and deformation behavior of cataclastic sandstone. Rock Mech. Rock Eng. http://dx.doi.org/10.1007/s00603-014-0623-8. Published online at http://link.springer.com/article/10.1007%2Fs00603-014-0623-8#page-1 on July 11, 2014.

Zhang, Y., Shao, J.F., Xu, W.Y., Jia, Y., Zhao, H.B., 2014b. Creep behaviour and permeability evolution of cataclastic sandstone in triaxial rheological tests. Eur. J. Environ. Civ. Eng. http://dx.doi.org/10.1080/19648189.2014.960103. Published online at http://www.tandfonline.com/doi/abs/10.1080/19648189.2014.960103#.VMsZIvRAXlA on September 19, 2014.

Zhang, Z.L., Xu, W.Y., Wang, W., 2012. Triaxial creep tests of rock from the compressive zone of dam foundation in Xiang-jiaba Hydropower Station. Int. J. Rock Mech. Min. Sci. 50 (1), 133−139. http://dx.doi.org/10.1016/j.ijrmms.2012.01.003.